To appear in Astrophysical Journal
Preprint typeset using LaTeX style emulateapj v. 04/17/13

A DIRECT STELLAR METALLICITY DETERMINATION IN THE DISK OF THE MASER GALAXY NGC4258

Rolf-Peter Kudritzki[1,2,3], Miguel A. Urbaneja[4], J. Zachary Gazak[1], Lucas Macri[5], Matthew W. Hosek Jr.[1], Fabio Bresolin[1], Norbert Przybilla[4]

To appear in Astrophysical Journal

ABSTRACT

We present the first direct determination of a stellar metallicity in the spiral galaxy NGC 4258 ($D = 7.6$ Mpc) based on the quantitative analysis of a low-resolution (~ 5 Å) Keck LRIS spectrum of a blue supergiant star located in its disk. A determination of stellar metallicity in this galaxy is important for the absolute calibration of the Cepheid Period-Luminosity relation as an anchor for the extragalactic distance scale and for a better characterization of its dependence as a function of abundance. We find a value 0.2 dex lower than solar metallicity at a galactocentric distance of 8.7 kpc, in agreement with recent H II region studies using the weak forbidden auroral oxygen line at 4363 Å. We determine the effective stellar temperature, gravity, luminosity and line-of-sight extinction of the blue supergiant being studied. We show that it fits well on the flux-weighted gravity–luminosity relation (FGLR), strengthening the potential of this method as a new extragalactic distance indicator.

Keywords: galaxies: distances and redshifts — galaxies: individual(NGC 4258) — stars: abundances — stars: early-type — supergiants

1. INTRODUCTION

The precise VLBI mapping of water masers orbiting the central black hole in NGC 4258 makes it possible to measure a geometrical distance to this spiral galaxy with unprecedented accuracy (Herrnstein et al. 1999; Humphreys et al. 2008). Most recently, Humphreys et al. (2013) have refined these measurements using a new model which includes disk warping and confocal elliptical maser orbits with differential precession. They obtained a distance of $7.60 \pm 0.17 \pm 0.15$ Mpc, where the uncertainties are split into formal fitting errors and a systematic term respectively.

Given such an accurate and precise distance, it is an obvious (though bold) step to use this galaxy as a new anchor point for extragalactic distance indicators, such as the Cepheid Period-Luminosity Relation (Leavitt & Pickering 1912, PLR). After the discovery with HST of a large sample of Cepheids by Macri et al. (2006), this galaxy was used by Riess et al. (2009) and Riess et al. (2011) as the first step in an HST survey for Cepheids in host galaxies of SNe Ia out to 30 Mpc, which resulted in a determination of the Hubble constant with a total uncertainty of 3.3%.

Simultaneously, there has also been a dramatic improvement in the measurement of the distance to the Large Magellanic Cloud. In a long-term project over eight years, Pietrzyński et al. (2013) accumulated photometric and spectroscopic observations of long-period, well-detached late-type eclipsing binaries to construct high-precision light and radial velocity curves of eight systems distributed along the line of nodes towards the LMC. The analysis of this unique observational material provided radius, extinction, luminosity and distance for each object resulting in a LMC distance with an unprecedented accuracy of 2%.

Combining the LMC and NGC 4258 as two anchor points of the extragalactic distance scale has the potential to further increase the robustness of the determination of the Hubble constant or, at least, to check for additional systematic effects. In the case of the PLR, HST studies of Cepheid fields at different galactocentric radii within spiral galaxies usually show that the variables in inner fields seem to be brighter by a few tenths of a magnitude than those in outer fields. This is usually interpreted as an effect of the metallicity gradient in spiral galaxies and a metallicity dependence of the PLR (Kennicutt et al. 1998; Freedman et al. 2001; McCommas et al. 2009; Gerke et al. 2011; Shappee & Stanek 2011). The Cepheids detected in the maser galaxy NGC 4258 also show such an effect (Macri et al. 2006). According to these studies, a difference between solar neighborhood metallicity and LMC metallicity of 0.4 dex will have an effect of 0.12 mag in distance modulus or 6% in distance, clearly too large if the ultimate goal is to measure a Hubble constant with a precision of 3% or better to constrain the equation of state of dark energy parameter w (see Macri et al. 2006 or Riess et al. 2011). While the interpretation of the physical reason of the brightness difference of inner and outer field Cepheids is heavily disputed (see Bresolin 2011, Kudritzki et al. 2012, Majaess et al. 2011, Storm et al. 2011) and while this effect might be less pronounced in the near-IR H-band used by Riess et al. (2011), it is very evident that a precise determination of distances using Cepheids should be accompanied by an accurate determination of stellar metallicities.

At distances significantly beyond the Magellanic Clouds, a direct determination of the metallicity of Cepheids based on spectroscopy is not possible. Instead, the work on the extragalactic distance scale cited above has used the oxygen abundance obtained from the strong emission lines of H II regions as a proxy for stellar metallicities. However, it has been shown over the last years (see Kudritzki et al.

[1] Institute for Astronomy, University of Hawai'i, 2680 Woodlawn Dr, Honolulu, HI 96822, USA
[2] University Observatory Munich, Scheinerstr. 1, D-81679 Munich, Germany
[3] Max-Planck-Institute for Astrophysics, Karl-Schwarzschild-Str.1, D-85741 Garching, Germany
[4] Institute for Astro- and Particle Physics, University of Innsbruck, Technikerstr. 25/8, A-6020 Innsbruck, Austria
[5] George P. and Cynthia Woods Mitchell Institute for Fundamental Physics and Astronomy, Department of Physics & Astronomy, Texas A&M University, 4242 TAMU, College Station, TX77843-4242, USA

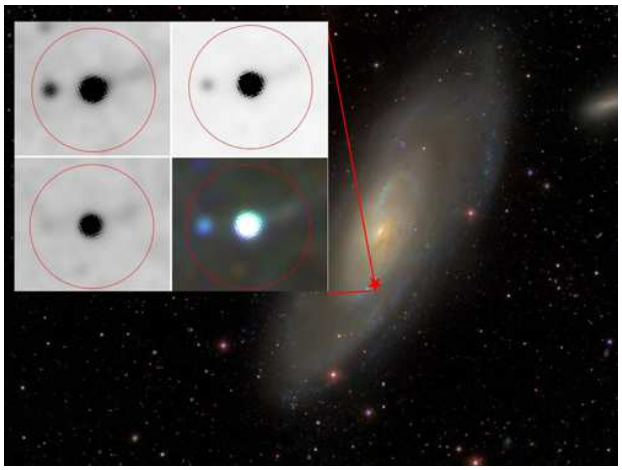

Figure 1. The location of the BSG target in NGC 4258 together with an enlarged B, V, I and RGN composite HST ACS image. The circle corresponds to 1 arcsec radius. For discussion of the second source see text.

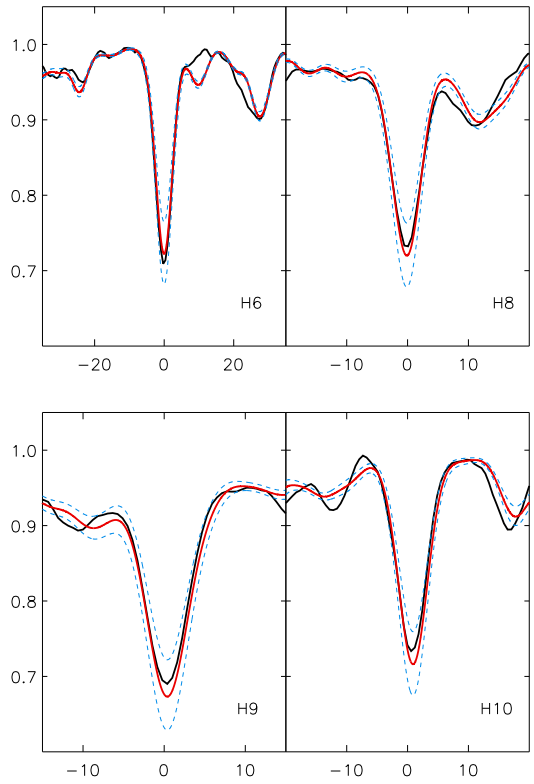

Figure 2. Fit of observed Balmer line profiles (black solid) with model atmospheres of T_{eff}=8300K and log g = 0.85 (red, solid) and 0.80 and 0.90 (both blue dashed), respectively. The gravity g is calculated in cgs units.

2008, Kewley & Ellison 2008, Bresolin et al. 2009, U et al. 2009, Kudritzki et al. 2012 for a detailed discussion) that these "strong-line methods" are subject to systematic uncertainties as large as 0.6 dex, which are poorly understood and can severely affect the inferred values of galaxy central metallicities and abundance gradients. This introduces an element of uncertainty in the use of Cepheids as extragalactic distance indicators, in particular, with the goal to obtain very accurate distances.

The important case of the maser galaxy is an illustrative example for this uncertainty. Macri et al. (2006) used oxygen abundances obtained from H II region strong line studies by Zaritsky et al. (1994) for their discussion of Cepheid metallicity in NGC 4258. These studies claim a very high central value of [O/H]=12+log(O/H)=9.17 and a rather steep gradient of -0.028 kpc^{-1}. On the other hand, the study by Bresolin (2011) included four H II regions with observations of the weak auroral [OIII] 4363 line, and determined a much lower central metallicity value of [O/H]=8.49 and a significantly shallower gradient of -0.010 kpc^{-1} (all values are taken from Bresolin 2011 but have been re-normalized to the new maser distance of 7.6 Mpc). At a galactocentric radius of 8.7 kpc (see below) this leads to a striking difference in oxygen abundance. Using the Zaritsky et al. result we obtain [O/H]=8.93, significantly larger than the solar value of [O/H]=8.69 (Allende Prieto et al. 2001; Asplund et al. 2009), whereas adopting the Bresolin result yields [O/H]=8.40 which is only slightly larger than the LMC value [O/H]=8.36 (also based on H II regions by Bresolin 2011). Obviously, when discussing Cepheid magnitude differences between NGC 4258 and the LMC, the question of whether the metallicity difference is 0.5 dex or almost zero is important.

While at the distance of the maser galaxy a direct spectroscopic investigation of Cepheid metallicities is not possible to settle this issue, there is an attractive alternative: the quantitative spectroscopy of blue supergiant stars (BSGs). BSGs are massive stars in the range between 15 and 40 $M_{\odot}$, which cross the Hertzpsrung-Russell diagram in 10^{4-5} yr from the main sequence to the red supergiant stage as stars of spectral type late B or A. Having an age of $\sim$ 10 million years, they belong to the same population as Cepheids albeit they are more massive and slightly younger. Their magnitudes can reach up to $M_V \cong -10$, rivaling the integrated brightness of globular clusters and dwarf spheroidal galaxies. They are more than four magnitudes brighter than Cepheids and, thus, perfect candidates for quantitative stellar abundance studies beyond the Local Group. Kudritzki et al. (2008) have shown that accurate metallicities based on elements such as iron, chromium, titanium etc. can be determined from low resolution spectroscopy of individual objects using refined NLTE model atmosphere diagnostic methods. This technique has now been applied on a variety of galaxy abundance studies (WLM – Bresolin et al. 2006; Urbaneja et al. 2008; NGC 3109 – Evans et al. 2007, Hosek et al. 2013; IC 1613 – Bresolin et al. 2007; M33 – U et al. 2009; NGC 300 – Kudritzki et al. 2008; M81 – Kudritzki et al. 2012).

The extension of this technique to the maser galaxy is a consequent next step. So far the most distant galaxy studied in the this way has been M81 with a distance of 3.5 Mpc. Investigating BSGs in NGC 4258 doubles the range in distance, which is a clear challenge pushing the method to a new limit. We have, thus, started a pilot project of multi-object spectroscopy of BSGs in this key galaxy for the extragalactic distance scale. In this paper, we present a first result, the direct determination of the metallicity of one BSG in NGC 4258 at a galactocentric distance of 8.7 kpc.

2. OBSERVATIONS AND DATA REDUCTION

Spectroscopic observations with one multi-object mask were carried out during the night of March 16, 2012, with the Keck 1 telescope on Mauna Kea and the Low Resolution Imaging Spectrograph (LRIS, Oke et al. 1995) using the atmospheric dispersion corrector, a slit width of 1.2 arcseconds, the D560 dichroic and the 600/4000 grism (0.63 Å pix^{-1}) and

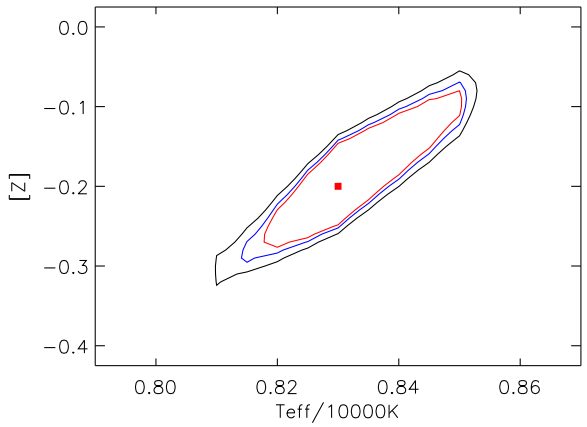

Figure 3. Isocontours $\Delta\chi^2$ of the metallicity [Z] and effective temperature T_{eff}fit of metal lines. The $\Delta\chi^2$ values of the isocontours are $\Delta\chi^2$=3 (red), 6 (blue), 12 (black), respectively.

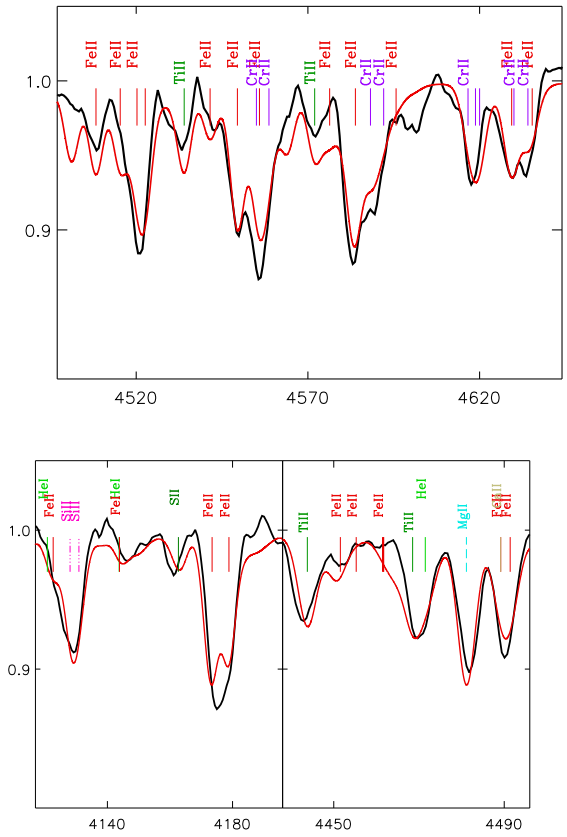

Figure 4. Observed metal line spectrum (black) in three spectral windows compared with a model spectrum (red) calculated for T_{eff}=8300K, log g=0.85 (cgs) and [Z]=-0.15.

the 900/5500 grating (0.53 Å pix^{-1}) in the blue and red channel, respectively. In this paper, we will discuss and analyze the blue channel (LRIS-B) spectra only, which have a resolution of 5 Å FHWM. One MOS field was prepared for this night with 23 targets. The BSG candidate targets were selected from an HST/ACS B, V, I survey of NGC 4258 (HST-GO-10802 and HST-GO-11570, P.I.: Adam Riess) that covers most of the disk of the galaxy in 17 fields. PSF photometry of all fields yielded 240 BSG candidates with -0.1 mag $\leq$ B-V $\leq$ 0.5 mag and V $\leq$ 22.0 mag (corresponding to $M_V \leq$-7.9 mag). Each candidate target was carefully inspected with regard to multiplicity. Targets for the mask were selected in a magnitude range from V = 20.4 to 22.0 mag to allow for a independent determination of distance using the FGLR-method (see below).

Unfortunately, the Keck observations were compromised by poor seeing of 1.3 arcsec (and sometimes worse) throughout the night. We have, therefore, restricted our investigation to the analysis of the brightest target (slit 6) with coordinates α(2000)=184.75836 and δ(2000)=+47.26312 and the following photometric properties: V=20.58 $\pm$ 0.02 mag , B-V=0.29 $\pm$ 0.05 mag, V-I=0.48 $\pm$ 0.03 mag in the Johnson-Cousins system. The deprojected galactocentric distance in units of the R_{25} radius is R/R_{25}=0.42 or (with R_{25}=20.6 kpc at a distance of 7.6 Mpc) corresponding to R=8.7 kpc (using the same de-projection as Bresolin 2011). Fig 1 shows the location of the target within NGC 4258 and a zoom of the HST ACS B, V, I images. The second source visible in these images is significantly fainter: V= 23.47 $\pm$ 0.06 mag, B-V= -0.11 ± 0.09 mag, V-I= -0.15 ± 0.10 mag. The LRIS slit was oriented perpendicular to the direction between the two sources to minimize contamination by the fainter star.

Nine MOS on-target exposures were taken each 45 minutes long. The extraction and reduction of the spectra was carried out in exactly the same way as described in Kudritzki et al. (2012). The final co-added and continuum normalized spectrum was smoothed over six pixels and has an average S/N level of 65.

3. SPECTROSCOPIC ANALYSIS

The basis for the the quantitative determination of stellar effective temperature, gravity and metallicity is a comprehensive grid of line-blanketed model atmospheres and very detailed NLTE line formation calculations of normalized spectra (for details, see Kudritzki et al. 2008, Kudritzki et al. 2012). Comparing calculated and observed spectra the spectral analysis proceeds in several steps. First, a fit curve in the (log g, $T_{\rm eff}$)-plane is constructed, along which the models reproduce the observed Balmer lines. At every $T_{\rm eff}$ the fit of the higher Balmer lines $H_{6,8,9,10}$ yields a value of gravity log g (see Fig 2) with an accuracy better than 0.05 dex. At lower $T_{\rm eff}$ the log g fit-values are lower, and they are higher at higher $T_{\rm eff}$ (typical Balmer line fit curves are shown in Kudritzki et al., 2008 or 2012). We do not use $H_{4,5}$ because these lines are contaminated by stellar wind and H II region emission. H_7 is blended by strong interstellar CaII.

In a next step, we move along this Balmer line fit curve in the (log g, $T_{\rm eff}$)-plane and compare at each $T_{\rm eff}$ the observed and calculated spectrum of metal lines in eight spectral windows. We split the spectrum in spectral windows for a piecewise accurate continuum normalization and to avoid Balmer lines, nebular emission lines and flaws in the spectrum. We then calculate a χ^2-value as a function of logarithmic metallicity relative to the sun [Z]=log $Z/Z_\odot$ and effective temperature $T_{\rm eff}$.

$$\chi^2([Z],T_{eff}) = (S/N)^2 \sum_{j=1}^{n_{pix}} (F_j^{obs} - F([Z],T_{eff})_j^{calc})^2 \qquad (1)$$

where S/N is the average signal-to-noise ratio per resolution element. The sum is extended over all spectral windows and n_{pix} is the sum of all pixel in all spectral windows. We then determine the minimum χ^2_{min} in the (log g, $T_{\rm eff}$)-plane and calculate $\Delta\chi^2$ isocontours around this minimum. In order to assess the uncertainty of this χ^2 fitting procedure we carry out extensive Monte Carlo calculations to determine which $\Delta\chi^2$ isocontour encloses 68% of the MC solutions obtained. We find that $\Delta\chi^2$=3 is a conservative estimate in reasonable agreement with statistical theory. More details describing the whole analysis process can be found in Hosek et al. (2013).

Fig 3 shows the isocontours in the (log g, $T_{\rm eff}$)-plane obtained for our BSG in this fitting process. From this figure we read off an effective temperature of $T_{\rm eff}$=8300^{+200}_{-100}K and a metallicity [Z]=-0.20±0.10. The gravity at the central fit point is log g = 0.85±0.05. Fig 4 displays fits of the metal lines with a model close to the final paramters of the fit in three spectral windows. Fig 5 (top) compares our stellar metallicity with the H II region results by Bresolin (2011).

Our analysis uses hydrostatic model atmospheres. This raises the question whether the abundance determination could be affected by a stellar wind. The effective temperature and gravity resulting from the analysis put the star relatively close to the Eddington-limit. As a consequence, it may have a strong stellar wind as known from other A-supergiants with similar stellar parameters (Kudritzki et al. 1999; McCarthy et al. 2006). However, detailed metal abundance studies using high spectral resulution and high S/N spectra of these objects have shown that their photospheric metal lines and the resulting abundances are not influenced by the outer atmosphere effects of stellar winds (Przybilla et al., 2006, 2008). Thus, while our low resolution spectra with the strongest Balmer lines $H_{\alpha,\beta}$ contaminated by H II emission do not allow to constrain the strength of the wind (note that objects of this type have low wind speeds of about 200 km/s only), we conclude that stellar wind effects are unlikely to affect our metallicity determination.

We can use the stellar parameters obtained in this way to calculate the intrinsic B-V and V-I colors of the BSG to determine the reddening. We obtain E(B-V)=0.20 mag and E(V-I)=0.34 mag. With E(B-V)=0.78E(V-I), we get E(B-V)=0.26 mag for the E(V-I) value determined. Thus, we adopt E(B-V)=0.23±0.03 mag for the reddening and with R_V=3.2 calculate A_V=0.73±0.10 mag for the extinction. With the distance modulus of m-M= 29.40 ± 0.07 mag to NGC 4258 and a bolometric correction from the model calculations of BC=-0.006 mag we finally obtain M_V=M_{bol}=-9.55±0.12 mag for the visual and bolometric magnitudes, respectively. The quoted uncertainty includes contributions from the photometry, extinction correction and distance modulus.

With stellar temperature and gravity determined BSGs can also be used as distance indicators using the flux-weighted gravity–luminosity relationship (FGLR) introduced by Kudritzki et al. (2003) and Kudritzki et al. (2008). The FGLR relates the flux-weighted gravity ($g_F \equiv g/T^4_{\rm eff}, T_{\rm eff}$ in units of 10^4K) of BSGs to their absolute bolometric magnitude M_{bol}

$$M_{\rm bol} = a(\log g_F - 1.5) + b \qquad (2)$$

with a = 3.41 and b = -8.02 as determined by Kudritzki et al. (2008). BSGs form such a relationship, because they evolve accross the HRD at roughly constant luminosity and mass.

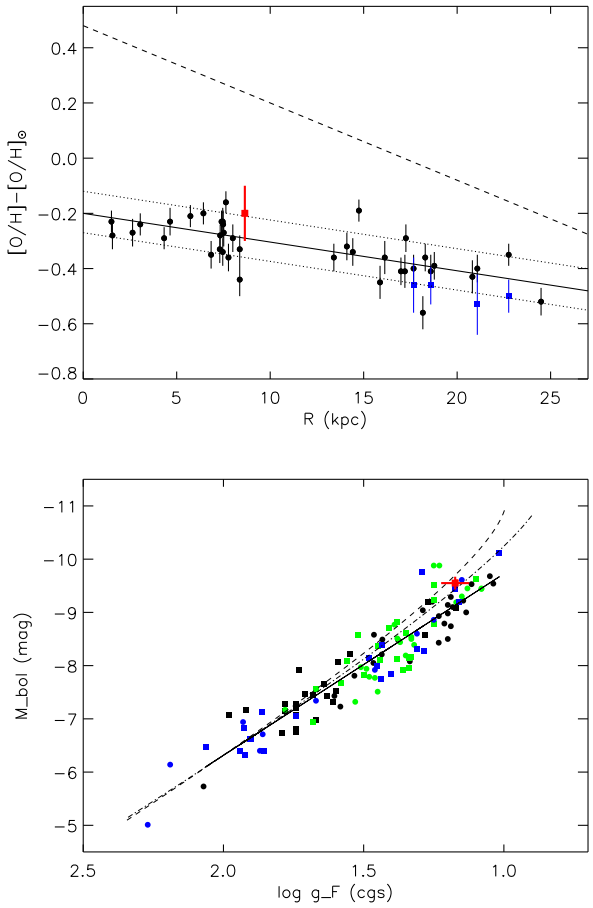

Figure 5. Top: Stellar Metallicity [Z] of the BSG (red) in NGC 4258 shown together with the H II region oxygen abundances by Bresolin (2011) as a function of galactocentric radius. The oxygen abundances are normalized to the solar value (see text). Black circles and blue squares correspond to strong line and auroral abundances respectively. The solid line is the Bresolin H II region abundance gradient regression (with ±1 σ shown dotted), whereas the dashed line represents the Zaritsky et al. (1994) abundance gradient and metallicity used in previous work (see text). Bottom: Flux weighted Gravity - luminosity relationship (FGLR) of BSGs observed in 11 galaxies (from Kudritzki et al. 2012 and Hosek et al. 2013) together with the calibration by Kudritzki et al. (2008) (solid) and the prediction by stellar evolution theory from evolutionary track by Meynet & Maeder (2005) including the effects of rotation for LMC (dashed-dotted) and SMC (dashed) metallicity. The BSG in NGC 4258 is shown in red.

As a consequemce, g_F remains constant during the horizontal HRD evolution independent of temperature, while at the same time the luminosity is a strong function of stellar mass and, therefore, g_F . Distance determinations using the FGLR have already been carried for a number of galaxies (see Kudritzki et al. 2012 and Hosek et al. 2013 and references, therein).

With only one object at this point no independent determination of the distance to NGC 4258 is possible. However, we can at least discuss the one observed BSG in the maser galaxy in relation to the objects already studied in other galaxies. This is done in Fig 5. The result is encouraging. While the object lies somewhat above the calibration relationship it is still within the observed scatter. Moreover, at the high luminosity end there is the prediction by stellar evolution theory of a possible curvature of the FGLR, for which we may already see an indication in the data observed (for a more detailed

discussion, see Hosek et al. 2013). Of course, this needs to be investigated by adding more BSGs belonging to NGC 4258 to the plot and by fitting a distance with less luminous objects. This work is presently under way.

4. DISCUSSION

In our spectroscopic analysis of a BSG at a galactocentric distance of 8.7 kpc we have found a stellar metallicity of -0.2 dex relative to the solar value. Given the uncertainty of 0.1 dex, this is in reasonable agreement with the recent H II region work by Bresolin (2011) which obtained a value of -0.29 ± 0.08 dex relative to solar at this galactocentric distance. While this is only the study of one object, it is already a strong confirmation that the stellar metallicity of the young population in the disk of NGC 4258 is very similar to that of the LMC, for which Romaniello et al. (2008) have found an average value of $[Z]_{LMC}$=-0.33 from a spectroscopic analysis of Cepheid variables (in perfect agreement with the H II region value of Bresolin 2011). Clearly, only by a study of a larger sample of BSGs in NGC 4258 covering a range of galactocentric distances will we be able to confirm whether the metallicity gradient is as shallow as found by Bresolin (2011) and the average metallicity clearly lower than solar. This work is presently under way.

The quantitative spectroscopy of the one object investigated so far has resulted in a bolometric magnitude and flux-weighted gravity in agreement with the FGLR of BSGs in galaxies. This is an encouraging first step towards a new calibration of this relationship in the maser galaxy NGC 4258 as a new anchor point of the extragalctic distance scale.

This work was supported by the National Science Foundation under grant AST-1008798 to RPK and FB. LMM acknowledges support by NASA through grants HST-GO-10802.14 and HST-GO-11570.09 from the Space Telescope Science Institute, which is operated by the Association of Universities for Research in Astronomy, Inc., under NASA contract NAS 5-26555; and by the Department of Physics & Astronomy at Texas A&M University through faculty startup funds and the Mitchell-Heep-Munnerlyn Endowed Career Enhancement Professorship in Physics or Astronomy.

The data presented in this work were obtained at the W.M. Keck Observatory, which is operated as a scientific partnership among the California Institute of Technology, the University of California and the National Aeronautics and Space Administration. The Observatory was made possible by the generous financial support of the W.M. Keck Foundation.

Based on observations made with the NASA/ESA Hubble Space Telescope, obtained from the Data Archive at the Space Telescope Science Institute, which is operated by the Association of Universities for Research in Astronomy, Inc., under NASA contract NAS 5-26555. These observations are associated with programs #10802 and #11570.

The authors wish to recognize and acknowledge the very significant cultural role and reverence that the summit of Mauna Kea has always had within the indigenous Hawaiian community. We are most fortunate to have the opportunity to conduct observations from this mountain.

Facilities: Keck (LRIS), HST (ACS).

REFERENCES

Allende Prieto, C., Lambert, D. L., & Asplund, M. 2001, ApJ, 556, L63
Asplund, M., Grevesse, N., Sauval, A. J., & Scott, P. 2009, ARA&A, 47, 481
Bèland, S., Boulade, O., & Davidge, T. 1988, Bulletin d'information du telescope Canada-France-Hawaii, 19, 16
Bresolin, F., Pietrzyński, G., Urbaneja, M. A., et al. 2006, ApJ, 648, 1007
Bresolin, F., Urbaneja, M. A., Gieren, W., Pietrzyński, G., & Kudritzki, R.-P. 2007, ApJ, 671, 2028
Bresolin, F., Gieren, W., Kudritzki, R.-P., et al. 2009, ApJ, 700, 309
Bresolin, F. 2011, ApJ, 729, 56
Cardelli, J. A., Clayton, G. C., & Mathis, J. S. 1989, ApJ, 345, 245
Evans, C. J., Bresolin, F., Urbaneja, M. A., et al. 2007, ApJ, 659, 1198
Freedman, W. L., Madore, B. F., Gibson, B. K., et al. 2001, ApJ, 553, 47
Gerke, J. R., Kochanek, C. S., Prieto, J. L., Stanek, K. Z., & Macri, L. M. 2011, arXiv:1103.0549
Herrnstein, J. R. et al. 1999, Nature, 400, 539
Hosek Jr., M. W., Kudritzki, R. P., Bresolin et al., 2013, ApJ, submitted
Humphreys, E. M. L., Reid, M. J., Greenhill, L. J., Moran, J. M., & Argon, A. L. 2008, ApJ, 672, 800
Humphreys, E. M. L., Reid, M. J., Greenhill, L. J., Moran, J. M., & Argon, A. L. 2013, ApJ, 775, 13
Kennicutt, R. C., Jr., Stetson, P. B., Saha, A., et al. 1998, ApJ, 498, 181
Kewley, L. J., & Ellison, S. L. 2008, ApJ, 681, 1183
Kudritzki, R. P., Urbaneja, M. A., Gazak, Z., et al. 2012, ApJ, 747, 15
Kudritzki, R. P., Urbaneja, M. A., Bresolin, F., et al. 2008, ApJ, 681, 269
Kudritzki, R. P., Bresolin, F., & Przybilla, N. 2003, ApJ, 582, L83
Kudritzki, R. P., Puls, J., Lennon, D. J., et al. 1999, A&A, 350, 970
Leavitt, H. S & Pickering, E. C. 1912, Harvard College Observatory Circular 173, 1
Macri, L. M., Stanek, K. Z., Bersier, D., Greenhill, L. J., & Reid, M. J. 2006, ApJ, 652, 1133
Majaess, D., Turner, D., & Gieren, W. 2011, ApJ, 741, L36
McCarthy, J. K., Kudritzki, R. P., Lennon, D., J., et al. 1997, ApJ, 482, 757
McCommas, L. P., Yoachim, P., Williams, B. F., et al. 2009, AJ, 137, 4707
Meynet, G. & Maeder, A. 2005, A&A, 429, 581
Oke, J. B. 1990, AJ, 99, 1621
Oke, J. B., Cohen, J. G., Carr, M., et al. 1995, PASP, 107, 375
Pietrzyński, G. et al. 2013, Nature, 495, 76
Przybilla, N., Butler, K., Becker, S. R., & Kudritzki, R. P. 2006, A&A, 445, 1099
Przybilla, N., Butler, K., & Kudritzki, R.-P. 2008, The Metal-Rich Universe, ed. G. Israelian, & G. Meynet (Cambridge: Cambridge University Press), 332
Riess, A. G., Macri, L., Casertano, S., et al. 2009, ApJ, 699, 539
Riess, A. G., Macri, L., Casertano, S., et al. 2011, ApJ, 730, 119
Romaniello, M., Primas, F., Mottini, M., et al. 2008, A&A, 488, 731
Schlegel, D. J., Finkbeiner, D. P., & Davis, M. 1998, ApJ, 500, 525
Shappee, B. J, & Stanek, K. Z., 2011, ApJ, 733, 124
Storm, J., Gieren, W., Fouque, P., et al. 2011, A&A, 534, 95
U, V., Urbaneja, M. A., Kudritzki, R.-P., et al. 2009, ApJ, 704, 1120
Urbaneja, M. A., Kudritzki, R.-P., Bresolin, F., et al. 2008, ApJ, 684, 118
Zaritsky, D., Kennicutt, R. C., Jr., & Huchra, J. P. 1994, ApJ, 420, 87